KCI Concrete Journal
Vol. 13 No. 2 pp. 67-74, July 2001

Damage Analysis of Reinforced Concrete Columns under Cyclic Loading

Jee-Ho Lee [1)]

[1)] Department of Civil and Environmental Engineering, Dongguk University, Korea

(Received May 18, 2001, Accepted July 19, 2001)

Abstract

In this study, a numerical model for the simulation of reinforced concrete columns subject to cyclic loading is presented. The model consists of three separate models representing concrete, reinforcing steel bars and bond-slip between a reinforcing bar and ambient concrete. The concrete model is represented by the plane stress plastic-damage model and quadrilateral finite elements. The nonlinear steel bar model embedded in truss elements is used for longitudinal and transverse reinforcing bars. Bond-slip mechanism between a reinforcing bar and ambient concrete is discretized using connection elements in which the hysteretic bond-slip link model defines the bond stress and slip displacement relation. The three models are connected in finite element mesh to represent a reinforced concrete structure. From the numerical simulation, it is shown that the proposed model effectively and realistically represents the overall cyclic behavior of a reinforced concrete column. The present plastic-damage concrete model is observed to work appropriately with the steel bar and bond-slip link models in representing the complicated localization behavior.

Keywords: reinforced concrete, damage, cyclic loading, degradation, bond slip, finite element method

1. Introduction

The computational simulation of damaged reinforced concrete members subject to cyclic and dynamic loading is important in the performance evaluation of newly designed and existing structures. For the accurate and reliable simulation of the damaged structural behavior, the effect of shear and bond-slip in the damage evolution should be modeled appropriately. In this study a numerical model for the simulation of reinforced concrete structures under the substantial amount of inelastic cyclic displacements is presented. The model consists of three separate models representing concrete, reinforcing steel bars and bond-slip between a reinforcing bar and ambient concrete or foundation anchorage.

The present concrete constitutive model is based on the plastic-damage model suggested by Lee and Fenves.[1] The plastic-damage model is derived from the Barcelona concrete model[2] by defining two damage variables, one for tensile damage and the other for compressive damage. The evolution equations for the hardening and degradation variables are obtained from the factorization of the stress strength function.

A simple and thermodynamically consistent degradation recovery scheme is introduced to simulate cracking closing and reopening. To ensure a well-posed structural system, a rate-independent version of the plastic-damage model is regularized by introducing a viscoplastic concept into the inelastic strain and degradation variables.

The cyclic behavior of longitudinal and transverse reinforcing steel bars is represented using the uniaxial inelastic model which includes the Bauschinger effect and the isotropic and kinematic hardening under large strain reversals. The bond-slip mechanism between a reinforcing bar and the ambient concrete is simulated using the nonlinear discrete bond-slip link model. Those three constitutive models are embedded in the corresponding finite elements to become the components of the present reinforced concrete model.

The proposed model is validated by comparing the numerical simulation of a reinforced concrete column under cyclic loads with the experimental result. Stress and strains of a reinforcing bar and bond-slip states at four observation times are presented to discuss on the evolution of bond stresses. The damage index contour plot is used to track the damage evolution in the concrete part of the column.

2. Plastic-Damage Model

In this chapter the plastic-damage model suggested by Lee and Fenves[1,3] for modeling cyclic behavior of concrete is outlined.

2.1 Constitutive Relationships

In the plastic-damage model, the stress $\boldsymbol{\sigma}$ is factored into the degradation damage, $(1-D)$, and the effective stress,

$$\begin{aligned}\bar{\boldsymbol{\sigma}} &= \mathbf{E}_0 : (\boldsymbol{\varepsilon} - \boldsymbol{\varepsilon}^p) \\ \boldsymbol{\sigma} &= (1-D)\bar{\boldsymbol{\sigma}} \\ &= (1-D)\mathbf{E}_0 : (\boldsymbol{\varepsilon} - \boldsymbol{\varepsilon}^p)\end{aligned} \tag{1}$$

where $\mathbf{E}_0$ is the initial elastic stiffness tensor, and $\boldsymbol{\varepsilon}^p$ is the plastic strain. The scalar variable D is assumed to represent the state of degradation damage on the stiffness:

$$\mathbf{E} = (1-D)\mathbf{E}_0$$

To model the different damage states for cyclic multiaxial loading, both the tensile damage variable κ_t and the compressive damage variable κ_c are used as independent damage indexes. Each damage variable is defined based on the ratio of dissipated plastic energy to the energy capacity per unit volume of materials (the specific fracture energy for tensile damage). To maintain objective results at the structural level, the characteristic length(l_t for tension, l_c for compression), which is the crack bandwidth along which the energy is dissipated, is specified as a material property. The factorization of the strength function into two functional forms, one for the effective stress and the other for the degradation damage variable, leads to the damage evolution equation described with the effective stress and damage variable vector $\boldsymbol{\kappa} = [\kappa_t \quad \kappa_c]^T$:

$$\dot{\boldsymbol{\kappa}} = \dot{\lambda}\mathbf{H}(\bar{\boldsymbol{\sigma}}, \boldsymbol{\kappa}) \tag{2}$$

The plastic strain rate is evaluated by the flow rule. In contrast with metals, a non-associative flow rule is necessary to obtain the proper dilatancy exhibited by frictional materials. If we use a Drucker-Prager type function as the plastic potential function for the present plastic-damage model, the plastic strain rate is derived from:

$$\boldsymbol{\varepsilon}^p = \dot{\lambda}\left(\frac{\mathbf{s}}{\|\mathbf{s}\|} + \alpha_p \mathbf{I}\right) \tag{3}$$

where λ is a non-negative function referred to as the plastic consistency parameter, $\|\mathbf{s}\| = \sqrt{\mathbf{s} : \mathbf{s}}$ denotes the norm of the deviatoric effective stress $\mathbf{s}$, and the parameter α_p is chosen to give the proper dilatancy for concrete.

For modeling the cyclic behavior of concrete, which has very different tensile and compressive yield strengths, it is necessary to use two cohesion variables in the yield function: c_t, a tensile cohesion variable, and c_c, a compressive cohesion variable. The yield function in Lubliner *et al.*[2], which only models isotropic hardening behavior in the classical plasticity sense, is modified to include two cohesion variables as follows:

$$F(\bar{\boldsymbol{\sigma}}, \boldsymbol{\kappa}) = \frac{1}{1-\alpha}\left[\alpha I_1 + \sqrt{3J_2} + \beta(\boldsymbol{\kappa})\langle \hat{\sigma}_{\max} \rangle - c(\boldsymbol{\kappa})\right] \tag{4}$$

where $\hat{\sigma}_{\max}$ denotes the algebraically maximum principal stress, and α is a parameter which is evaluated by the initial shape of the yield function. The evolution of the yield function is determined by defining β, which is a constant in the original Lubliner's model, and the cohesion parameter, c, such that:

$$\begin{aligned}\beta &= \frac{c_c(\boldsymbol{\kappa})}{c_t(\boldsymbol{\kappa})}(1-\alpha) - (1+\alpha) \\ c &= c_c(\boldsymbol{\kappa})\end{aligned} \tag{5}$$

Fig. 1 shows the initial shape of the yield surface, $F(\bar{\boldsymbol{\sigma}}, \mathbf{0}) = 0$, in the principal plane stress space. In Figure 1, β_0 and c_0 denote β and c, respectively, at the undamaged initial state.

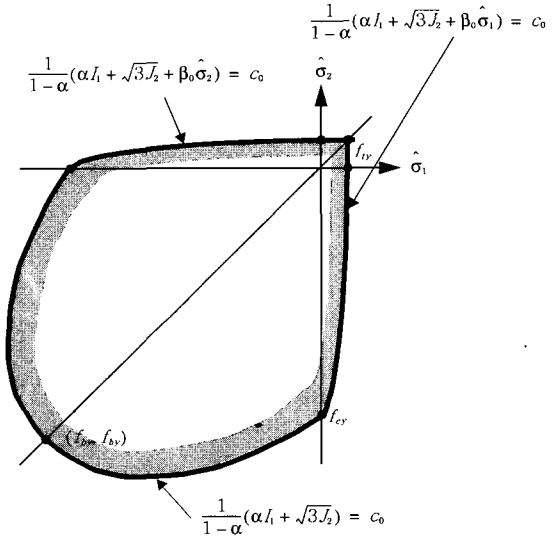

Fig. 1 Yield function of plastic-damage model

2.2 Stiffness Degradation and Crack Opening / Closing

The experimental cyclic tests of concrete demonstrate that the degradation of stiffness from microcracking occurs in tension and compression becomes more significant as the strain increases. The mechanism of stiffness degradation under cyclic loading is complicated because of the opening and closing of microcracks. The crack opening/closing behavior can be modeled as elastic stiffness recovery during elastic unloading from a tensile state to a compressive state. Using a multiplicative parameter $0 \le s \le 1$ on the tensile degradation variable D_t, we have the degradation damage variable $D = 1-(1-D_c(\kappa))(1-sD_t(\kappa))$, where D_c is the compressive degradation variable. Accordingly, the total stress σ is written as:

$$\sigma = (1-D_c(\kappa))(1-sD_t(\kappa))\mathbf{E}_0 : (\varepsilon - \varepsilon^p) \tag{6}$$

where $\mathbf{E}_0$ is the initial elastic stiffness tensor. The parameter s is chosen to represent the stiffness recovery as follows:

$$s(\bar{\sigma}) = \frac{\sum_{i=1}^{3}\langle\hat{\bar{\sigma}}_i\rangle}{\sum_{i=1}^{3}|\hat{\bar{\sigma}}_i|}$$

After a large amount of microcracking, the crack opening and closing mechanism becomes similar to discrete cracking, which cannot be represented by the classical approach of the inelastic strain evolution. The modified evolution relation in Lee and Fenves[3] is used to simulate large crack opening and the closing/reopening process in the continuum context. It can be assumed that the microcracks are joined to construct a discrete crack if $\kappa_t \ge \kappa_{cr}$, where κ_{cr} is an empirical value near unity. At that tensile damage level, the evolution of the plastic strain caused by the tensile damage is stopped.

2.3 Rate-Dependent Regularization

The modeling of softening as well as hardening behavior is important for realistic static and dynamic analyses of concrete structures. Unfortunately, representing the softening behavior with a model based on rate-independent plasticity makes the governing initial-boundary value problem become ill-posed such that a unique solution may not exist.[4,5] In most cases, uniqueness is not guaranteed in softening regions and, with a non-associative flow rule, even in hardening regions.[6] A numerical solution for an ill-posed initial-boundary value problem cannot guarantee a unique converged solution and the results show a strong dependency on mesh refinement and alignment. This singularity can be regularized using viscoplasticity by imposing weaker plastic consistency condition around the yield surface.

In the present plastic-damage model, the regularization scheme based on the Duvaut-Lions viscoplastic model[7] is applied to the rate-independent plastic strain and degradation damage variable:

$$\begin{aligned}\dot{\varepsilon}^i &= \frac{1}{\mu}(\varepsilon^p - \varepsilon^i)\\ \dot{\bar{D}} &= \frac{1}{\mu}(D - \bar{D})\end{aligned} \tag{7}$$

where μ is the viscosity parameter and $\bar{D}$ is a viscously regularized degradation variable. Accordingly, the stress-strain relation in Eq. (1) is restated using the new rate-dependent variables in Eq. (7) as:

$$\sigma = (1-\bar{D})\mathbf{E}_0 : (\varepsilon - \varepsilon^i) \tag{8}$$

The complete description of the rate-dependent plastic-damage model is found in Lee and Fenves.[3]

2.4 Cyclic Loading Example

Performance of the present plastic-damage model in representing the cyclic behavior of plain concrete is demonstrated by comparing numerical results with the existing experimental data : Gopalaratnam and Shah[8] and Karsan and Jirsa[9]. The loads are applied by displacement control, and for all cases Poisson's ratio is 0.18. The following material properties are used : 1) for cyclic tensile case, $E_0 = 3.1\times10^4$ MPa, $f_t' = 3.48$ MPa, $G_t = 12.3$ N/m, $l_t = 25.4$ mm, $\alpha_p = 0.23$; and 2) for cyclic compressive case, $E_0 = 3.17\times10^4$ MPa, $f_c' = -27.6$ MPa, $G_c = 17500$ N/m, $l_c = 25.4$ mm, $\alpha_p = 0.23$. Fig. 2 shows the simulated tensile and compressive stress-strain behaviors respectively. The numerical simulations represent the experimental results very well. For both cases the degradation of stiffness is simulated at each unloading/reloading cycle as well as the softening behavior.

3. Components of RC Model

In this chapter, three components of the proposed reinforced concrete model are discussed in the context of the finite element method.

3.1 Concrete

The concrete model plays a crucial role in the finite ele-

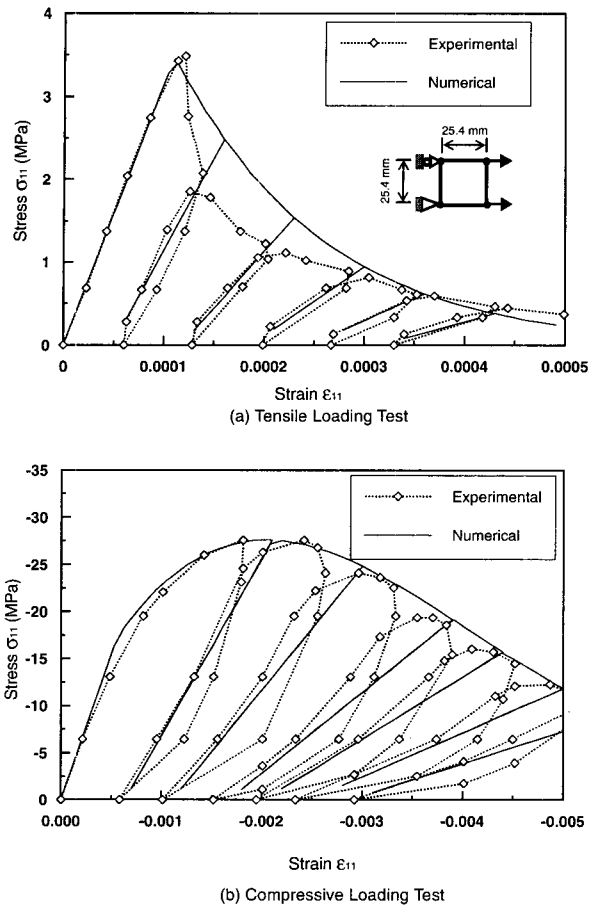

Fig. 2 Numerical simulation of cyclic uniaxial loading tests compared with experimental results

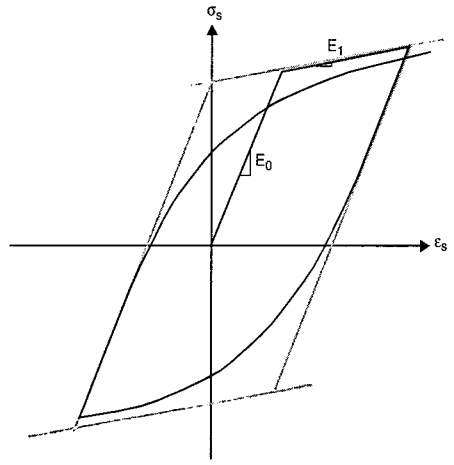

Fig. 3 Stress-strain relation of steel

ment analysis of reinforced concrete structures because it must represent initiation and localization of tensile cracking and compressive crushing damage. The plastic-damage model described in the previous sections is used to represent nonlinear concrete behavior including material hardening and softening, stiffness degradation, and stiffness recovery on crack closing. Ductility increase of confined concrete compressive parts can be modeled using the properly increased value of the compressive counter part of the fracture energy, which is the area of the compressive stress-plastic strain curve. As shown earlier, the plastic-damage model effectively reproduces the realistic concrete behavior under monotonic and cyclic loading. Those constitutive relations of the plastic-damage model are embedded in plane stress quadrilateral elements.

3.2 Reinforcing Steel Bar

To represent the behavior of the reinforcing bar under cyclic loading, a material model should include the constitutive relations of the isotropic and kinematic hardening, and the Bauschinger effect. In the Menegotto and Pinto model,[10] the stress-strain relation is defined based on a curvature parameter to reproduce the realistic shape of the transition curve and the Bauschinger effect. Filippou *et al.* [11] proposed a modified version of the Menegotto and Pinto model to incorporate the isotropic hardening effect in the original model In this study, the modified model is used for the uniaxial constitutive relation of longitudinal and transverse steel reinforcement (Fig. 3).

The constitutive model for the steel reinforcement is implemented in truss elements to represent reinforcing bars separately from concrete. This approach gives better representation for the cracked reinforced concrete body than the so-called embedded model, in which reinforcing bars are included in a concrete element internally, because the present model can simulate more damaged modes using the separate constitutive models.

3.3 Bond-Slip Link

In most cases, a reinforcing bar and ambient concrete are not perfectly bonded each other. The bond-slip mechanism between concrete and reinforcing bars becomes more important under large displacement loading because it significantly affects on the contribution of reinforcing bars to the overall structural response.

In this study, the bond-slip mechanism is represented using the discrete link model described in Eligehausen *et al.*.[12] A combination of multi-linear and exponential functions is used for the smooth representation of bond stress loading curves as shown in Fig. 4. The large amount of slip during unloading is included in the model.

The bond-slip link constitutive model is implemented in zero-length truss elements which connect reinforcing bar elements to surrounding concrete elements. Slip is supposed to take place only along the longitudinal direction of a reinforcing bar, and transverse directional slip is constrained by imposing large stiffness for that direction.

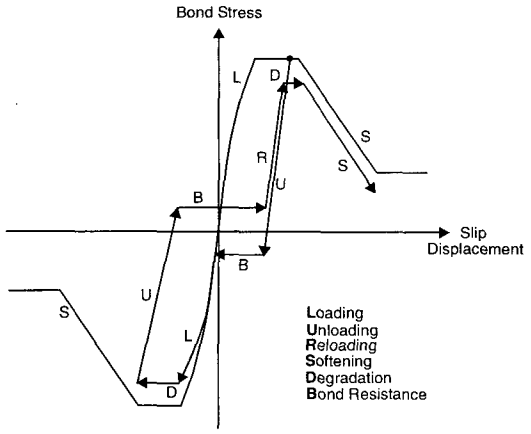

Fig. 4 Loading/unloading in bond stress-slip relation

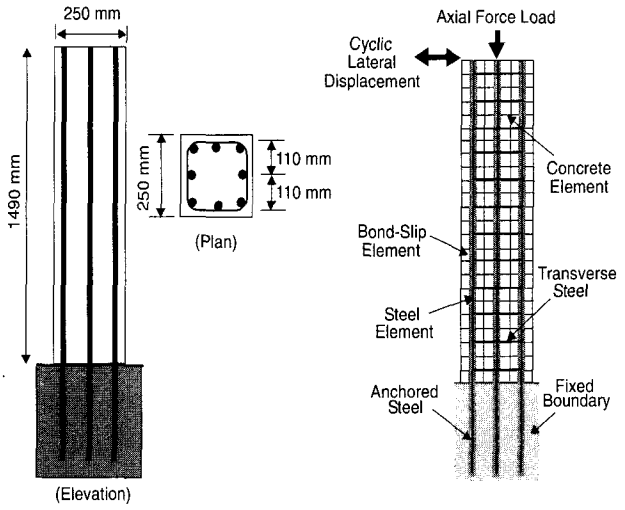

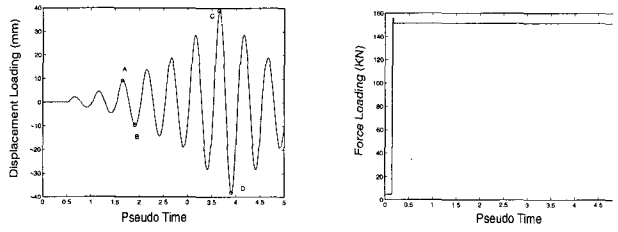

Fig. 5 Geometry, finite element mesh and loads

4. Column Analysis

A cyclically loaded reinforcing concrete column is tested to demonstrate performance of the present reinforced concrete model. The geometry description and finite element mesh of the column tested by Bousias *et al.* [13] are illustrated in Fig. 5(a) and (b). The column is 1490mm long with 15mm covers in all directions and anchored. All eight longitudinal reinforcing bars are 16mm in diameter. There are also transverse steel bars to confine concrete.

The test column is modeled using the present RC model, and implemented in the finite element program FEAP.[14] For concrete four-node quadrilateral isoparametric plane stress elements with 2-by-2 Gauss integration are used. The longitudinal steel bars are connected to the concrete elements through the bond-slip link elements, while the transverse bars are directly connected to the plane concrete elements because slip of a transverse steel bar is negligible.

All longitudinal steel bars are extended to the anchorage foundation, which is modeled using the rigid boundary condition in this study. The bond-link elements connect the steel bars located in the foundation to the fixed points in the rigid anchorage to simulate the bond-slip behavior in the anchorage foundation.

The amount of the steel used for the experimental test is converted for the appropriate plane stress computation considering the sectional area of the steel bars and the thickness of the concrete column. The converted sectional areas of the outside and outside longitudinal steel bars are 2.45 mm^2 (representing three reinforcing bars), and 1.64 mm^2 (representing two reinforcing bars), respectively. The converted sectional area of the transverse steel bars is 0.4 mm^2 for each corresponding truss element.

For the computational simulation of the experimental test[13] the following material properties are used: 1) for concrete, $E_0 = 1.7\times10^4$ MPa, $f_t' = 3$ MPa, $G_t = 1$ N/mm, $f_c' = 30$ MPa, $G_c = 100$ N/mm for unconfined concrete, $G_c = 200$ N/mm for confined concrete, $\alpha_p = 0.2$, Poisson's ratio is 0.18; and 2) for reinforcement steel, $E_0 = 20\times10^4$ MPa, $f_{sy} = 460$ MPa, Poisson's ratio is 0.2. 3) for bond-slip link, the initial yield stress = 5MPa, the initial yield slip displacement = 0.3 mm. The element size is used for the tensile and compressive characteristic length scales in each element to represent the crack bandwidth properly in this kind of quasi-static problem. The horizontal cyclic displacement control and the axial force loading, plotted in Fig. 5(c) and (d), respectively, are applied. Four observation times are marked as A, B, C and D in Fig. 5(c) and Fig. 6(a) in the load-displacement plot.

Fig. 6 (b) shows the computed hysteretic load-displacement curve at the top of the column compared with the experimental response. The results show that the proposed model can realistically simulate the nonlinear load-displacement response of a reinforced concrete structure under cyclic loading. The crack opening and closing is properly represented through the stiffness degradation and recovery relation. It also shows outstanding performance of the present model in reproducing the pinching effect during un loading and reloading following the substantial displacement loading path. It is observed that the numerical model can realistically simulate the cyclic response of the column in the substantial displacement loading range, where the tensile strength of

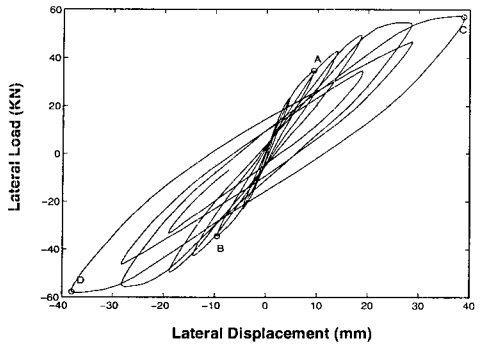

(a) Load vs Displacement History from Experiment

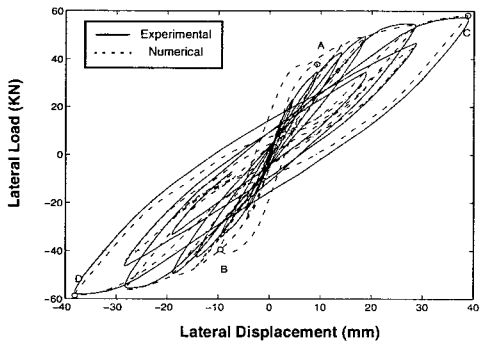

(b) Numerical Simulation of Experimental Lateral Load-Displacement Relationship

Fig. 6 Numerical result compared with experimental result

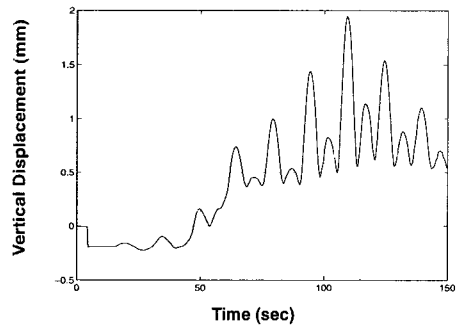

(a) Center Point Vertical Displacement History at Column Top

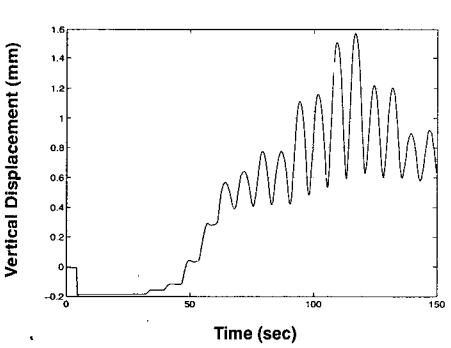

(b) Average Vertical Displacement History at Column Top

Fig. 7 Vertical displacement history

localized regions is dominated by bond-slip mechanism.

The evolution of the vertical displacement at the column top is plotted in Fig. 7. Fig. 7(a) shows the vertical displacement change at the center of the column top and Fig. 7(b) shows the average value of all vertical displacement changes over the column top. The permanent axial compressive deformation due to the axial load is on set instantly at the initial stage and increases gradually. This deformation is partly recovered in periodic pattern as the column is bent in either direction. In the experimental test,[13] a similar result for axial deformation evolution is observed.

In Fig. 8 the sectional force and the strain distribution curves along the left reinforcing bar are plotted. It is noted that the sectional force in Fig. 8(a) is calculated for the converted cross section of the steel bars, which are represented as a single truss element in the present model. The strain of the steel bar is concentrated near the column base, where the concrete damage is localized.

The evolution curves of the bond force and the slip displacement between the reinforcing bar and the ambient concrete at the four observation times are calculated and plotted at Fig. 9(a) and (b), respectively. The directions of the bond force and the slip displacement are changed near the column base, which means, along with the curves in Fig. 8, that the present model gives realistically simulated results for the damaged reinforced concrete composite under cyclic loading.

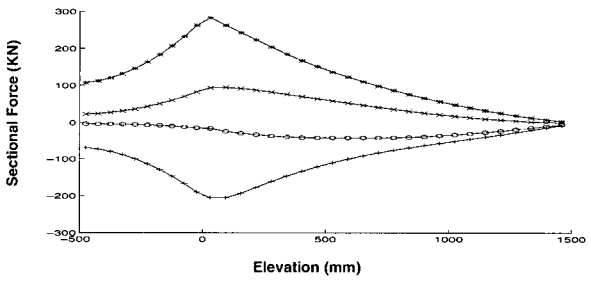

(a) Evolution of Sectional Force Distribution in Reinforcing Bar

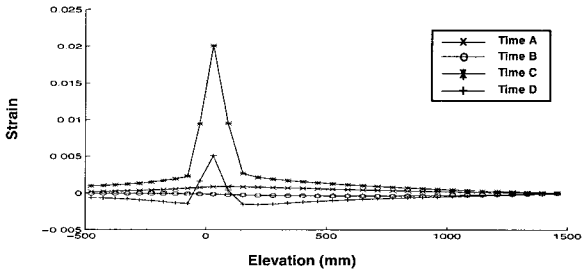

(b) Evolution of Strain Distribution in Reinforcing Bar

Fig. 8 Evolution of sectional force and strain in reinforcing bar

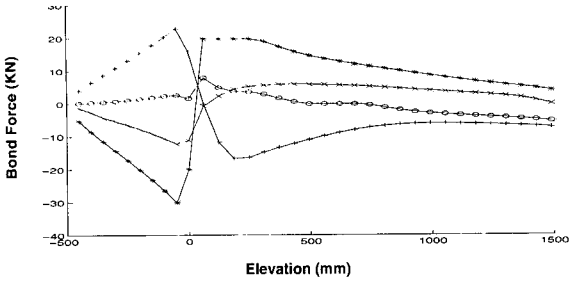

(a) Evolution of Bond Force Distribution

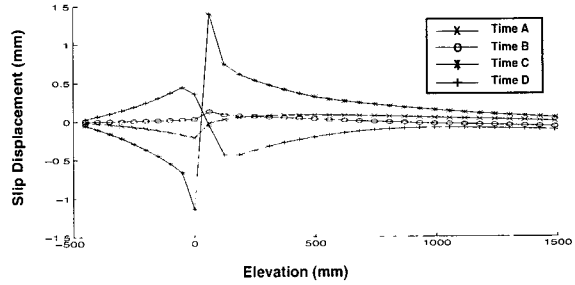

(b) Evolution of Slip Displacement

Fig. 9 Evolution of bond force and slip displacement

Contour plots for the tensile damage evolution at the four observation times are shown in Fig. 10. The area where the tensile damage variable is close to 1 represents substantially cracked zone. In Fig. 11, the simulation of crack opening and closing is demonstrated as evolution contours of the degradation variable. The total or partial recovery of stiffness at the cracked bottom corners of the column is observed in Fig. 11(c) and (d).

5. Conclusions

In this study, a model for the simulation of reinforced concrete structures subject to cyclic loading is presented. The model is based on three constitutive models representing the components of a reinforced concrete composite body: concrete, reinforcing steel and bond-slip. The plastic-damage model is used to simulate the inelastic behavior of damaged concrete including stiffness degradation and crack opening/closing. The nonlinear steel bar model based on the Menegotto and Pinto model is used for longitudinal and transverse reinforcing bars. Bond-slip mechanism between a reinforcing bar and ambient concrete is reproduced using the hysteretic bond-slip link model. Those three constitutive models are embedded in the corresponding finite elements and connected in finite element mesh to represent a reinforced concrete structure.

From the numerical simulation, we can conclude that the proposed model effectively and realistically represents the

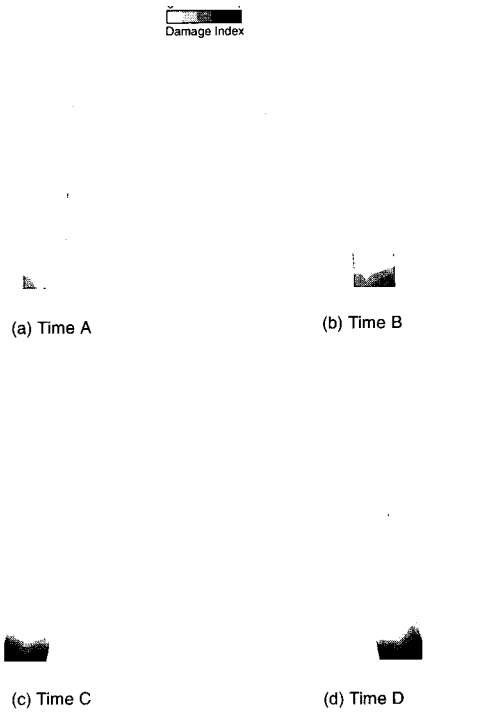

(a) Time A (b) Time B

(c) Time C (d) Time D

Fig. 10 Evolution of tensile damage variable

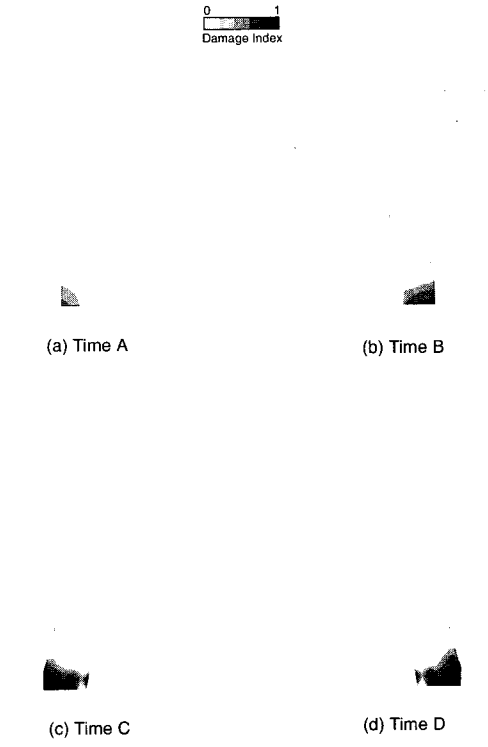

(a) Time A (b) Time B

(c) Time C (d) Time D

Fig. 11 Evolution of degradation damage variable

overall cyclic behavior of a reinforced concrete column. The present plastic-damage concrete model is observed to work appropriately with the steel bar and bond-slip link models in representing the complicated localization behavior including the strain concentration and excessive slip of the reinforcing bars in substantially damaged areas.

Acknowledgements

This work has been supported by the Dongguk University research fund. The writer thanks Professors Gregory L. Fenves and Filip C. Filippou for helpful discussions.

References

1. Lee, J., and Fenves, G. L., "Plastic-Damage Model for Cyclic Loading of Concrete Structures," Journal of Engineering Mechanics, ASCE, Vol. 124, No. 8, 1998, pp. 892-900.
2. Lubliner, J., Oliver, J., Oller, S., and Onate, E., "A Plastic-damage Model for Concrete," International Journal of Solids and Structures, Vol. 25, No. 3, 1989, pp. 299-326.
3. Lee, J., and Fenves, G. L., "A Plastic-Damage Concrete Model for Earthquake Analysis of Dams," Earthquake Engineering and Structural Dynamics, Vol. 27, 1998, pp. 937-956.
4. Needleman, A., "Material Rate Dependence and Mesh Sensitivity in Localization Problems," Computer Methods in Applied Mechanics and Engineering, Vol. 67, 1988, pp. 69-85.
5. Bigoni, D., and Hueckel, T., "Uniqueness and localization - I. Associative and Non-Associative Elastoplasticity," International Journal of Solids and Structures, Vol 28, 1991, pp. 197-213.
6. Sandler, I. S., and Pucik, T. A., "Non-uniqueness in dynamic rate-independent non-associated plasticity," in G. Z. Voyiadjis et al. (eds), Mechanics of Materials and Structures, 1994, pp. 221-240.
7. Duvaut, G., and Lions, J. L., Inequalities in Mechanics and Physics (translated from the French by C. W. John), Springer-Verlag, NY, 1976.
8. Gopalaratnam, V. S., and Shah, S. P., "Softening Response of Plain Concrete in Direct Tension," ACI Journal, Vol. 82, No. 3, 1985, pp. 310-323.
9. Karsan, I. D., and Jirsa, J. O., "Behavior of Concrete under Compressive Loadings," Journal of the Structural Division, ASCE, Vol. 95, No. ST12, 1969, pp. 6935-2563.
10. Menegotto, M., and Pinto, P. E., "Method of Analysis for Cyclically Loaded Reinforced Concrete Plane Frames Including Changes in Geometry and Non-Elastic Behavior of Elements under Combined Normal Force and Bending," Proceedings, IABSE Symposium on Resistance and Ultimate Deformability of Structures Acted on by Well Defined Repeated Loads, Lisbon, 1973, pp. 15-22.
11. Filippou, F. C., Popov, E. P., and Bertero, V. V., "Effects of Bond Deterioration on Hysteretic Behavior of Reinforced Concrete Joints," EERC Report 83-19, Earthquake Engineering Research Center, University of California, Berkeley, California, 1983.
12. Eligehausen, R., Popov, E. P., and Bertero, V. V., "Local Bond Stress-Slip Relationships of Deformed Bars Under Generalized Ecxitations," EERC Report 83-23, Earthquake Engineering Research Center, University of California, Berkeley, California, 1983.
13. Bousias, S. N., Verzeletti, G., Fardis, M. N., and Guitierrez, E., "Load-Path Effects in Column Biaxial Bending and Axial Force," Journal of Engineering Mechanics, ASCE, Vol. 125, No. 5, 1995, pp. 596-605.
14. Taylor, R. L., FEAP: A Finite Element Analysis Program (Version 5.01 Manual), Department of Civil Engineering, University of California, Berkeley, California, 1996.